

# New banana-shaped thiobenzoate liquid crystals with B6, B1 and B2 phases

J. C. Rouillon,<sup>a</sup> J. P. Marcerou,<sup>a</sup> M. Laguerre,<sup>b</sup> H. T. Nguyen<sup>a</sup> and M. F. Achard<sup>\*a</sup>

<sup>a</sup>Centre de Recherche Paul Pascal, CNRS, Université Bordeaux I, Av. A. Schweitzer, 33600 Pessac, France. E-mail: achard@crpp.u-bordeaux.fr

<sup>b</sup>Institut Européen de Chimie et Biologie, Ecole Polytechnique–Université Bordeaux I–Université Bordeaux 2, Avenue Pey-Berland, 33007 Pessac, France

Received 6th April 2001, Accepted 8th August 2001

First published as an Advance Article on the web 1st October 2001

A new series of achiral banana-shaped compounds (“S<sub>n</sub>”) has been synthesised and studied by the classical techniques (optical microscopy, differential scanning calorimetry, X-ray diffraction and electro-optic investigations). The short homologues (S<sub>6</sub>, S<sub>7</sub>) present an intercalated smectic B6 and a two-dimensional B1 phase. The intermediate S<sub>8</sub>–S<sub>10</sub> compounds only form a B1 phase while the mesophase of long homologues (S<sub>11</sub>–S<sub>16</sub>) is identified as a switchable smectic B2 mesophase.

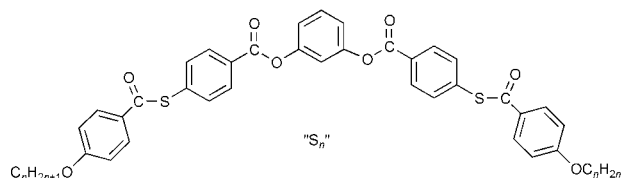
## Introduction

Liquid crystals formed by bent-shaped molecules represent a growing topic in liquid crystal research. These materials form new smectic and two-dimensional phases which are unlike those obtained from normal calamitic molecules.<sup>1</sup> Such banana compounds have attracted considerable interest because of their unexpected electro-optical properties.<sup>2</sup> Indeed, as a result of the bent shape, a polar order within the smectic layers can be induced and some phases exhibit ferro- or antiferroelectric properties although the molecules are non-chiral. We use in this paper the nomenclature “B<sub>n</sub> phases” (B1–B7) suggested at the workshop on Banana-Shaped Liquid Crystals: Chirality by Achiral Molecules, held in Berlin in 1997 even if this nomenclature must be considered as preliminary since, in several cases, the assignment is only based on similar textures and not on similar structures. For example, the B7 one probably has to be divided into subclasses, while the B2 one has been associated with the coexistence of chiral and racemic states in pure compounds.<sup>6</sup> This fluid smectic referred to as the “B2 phase”<sup>3–7</sup> presents an antiferroelectric switching. The B5 smectic phase possesses an additional short range order within the layers but keeps the same electrooptic response.<sup>5</sup> An intercalated smectic phase labelled as B6,<sup>1</sup> with a layer spacing smaller than the half-length of the molecule, has been observed in one compound but no electro-optic response has been evidenced. We recently found a bilayer smectic phase with an antiferroelectric-like response (designated as B8) and a bilayer–monolayer phase transition was observed in one compound.<sup>8</sup> The B7 labelling undoubtedly corresponds to different phases all exhibiting the characteristic textures observed in the original B7 of nitro compounds.<sup>9</sup> This first B7 exhibits a complex bidimensional structure and no electrical response. We recently reported another variant of B7 (B7<sub>bis</sub>) with a two-dimensional structure and a ferro-type response.<sup>10</sup> Materials with a lateral fluoro substituent on the external phenyl rings,<sup>11</sup> or with sulfur containing tails<sup>12</sup> exhibit a smectic phase with “B7 textures”, and with an antiferroelectric switching. Recently, a ferro-type response has been reported for bent-shaped compounds with a chiral terminal chain.<sup>13</sup>

In all these cases, these five-ring banana-shaped liquid crystals present azomethine groups which are not very stable to moisture and high temperature. Thus we prepared different materials without these groups and some of them are able to

form liquid crystalline phases. For example, series based on the ester of isophthalic acid as the central core and with thiocarboxylic linkages form nematic and smectic C phases.<sup>14</sup> The introduction of a fluorine atom on the external phenyl rings induces a complex smectic polymorphism with four successive switchable smectic phases<sup>14</sup> which appear different from the known B<sub>n</sub> phases.

We present here another series of banana compounds with thiocarboxylic connecting groups. These molecules are derived from resorcinol as the central core in contrast with the series previously reported in ref. 14 which are based on isophthalic acid. These new symmetric banana-shaped molecules correspond to the formula:

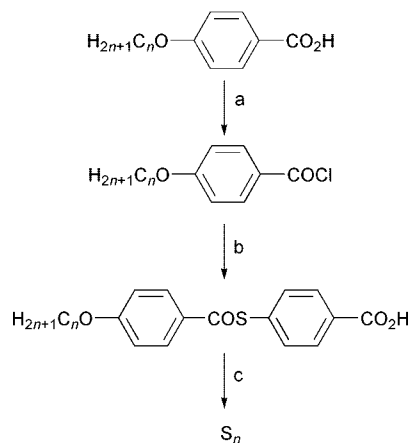


The materials are labelled “S<sub>n</sub>”, where *n* is the number of carbon atoms in the terminal ether chain (*n* = 6–16). In these molecules the ester groups are linked to the 1,3 positions of the central phenyl ring and the thiobenzoate groups are placed between the outside phenyl rings. They differ from the thiobenzoate series reported in ref. 14 by the direction of the connecting benzoate groups which are reversed.

## Synthesis

The synthesis of the new banana-shaped liquid crystals is outlined in Scheme 1.

First the appropriate 4-*n*-alkoxybenzoic acid is converted to its acid chloride which is in turn reacted with 4-mercapto-benzoic acid in the presence of a base: triethylamine. The acid terminated thiobenzoate intermediate is then esterified with resorcinol in the presence of 1,3-dicyclohexylcarbodiimide (DCC) and dimethylaminopyridine (DMAP) as catalyst in a solvent (dichloromethane). All the liquid crystals were purified by chromatography on silica gel using dichloromethane as eluent followed by recrystallization from an ethanol–toluene mixture.



**Scheme 1** Reagents and conditions: a,  $(\text{COCl})_2$ ,  $\text{CH}_2\text{Cl}_2$ ; b, 4-HS-Ph-COOH,  $\text{Et}_3\text{N}$ ,  $\text{CH}_2\text{Cl}_2$ ; c, resorcinol, DCC, DMAP,  $\text{CH}_2\text{Cl}_2$ .

4-[(4'-Tetradecyloxybenzoyl)sulfanyl]benzoic acid: a solution of 4-tetradecyloxybenzoyl chloride (3.7 g, 10 mmol, prepared from the corresponding acid and oxalyl chloride) and 4-mercaptobenzoic acid (1.57 g, 10 mmol) was prepared in dichloromethane (50 ml). To this stirred solution was then added triethylamine (1.2 g, 12 mmol) over about five minutes. The resulting solution was stirred overnight and then concentrated to dryness by rotatory evaporation. The resultant solid was hydrolysed with dilute aqueous hydrochloric acid and extracted with ethyl acetate (300 ml). The organic solution was dried over anhydrous  $\text{Na}_2\text{SO}_4$  and the solvent was evaporated. The solid was recrystallised from ethyl acetate. Yield: 2.6 g (61%); NMR  $^1\text{H}$  ( $\text{CDCl}_3$ , ppm): 0.9 (t, 3H,  $\text{CH}_3$ ), 1.1–2.1 (m, 2H, 12  $\text{CH}_2$ ), 4.1 (t,  $\text{CH}_2\text{O}$ ), 6.9–8.4 (m, 8H, Ar).

1,3-Phenylene bis{4-[(4'-tetradecyloxybenzoyl)sulfanyl]benzoate}: to a solution of resorcinol (110 mg, 1 mmol), DCC (440 mg, 2.2 mmol) and DMAP (20 mg) in 20 ml of dichloromethane, was added 4-[(4'-tetradecyloxybenzoyl)sulfanyl]benzoic acid (1.05 g, 2.2 mmol). The mixture was stirred overnight at room temperature. The solvent was evaporated and the solid was purified by chromatography on silica gel with dichloromethane as solvent. The pure product was then evaporated and finally recrystallised in an ethanol–toluene mixture. Yield: 0.52 mg (51%); NMR  $^1\text{H}$  ( $\text{CDCl}_3$ , ppm): 0.9 (t, 6H, 2  $\text{CH}_3$ ), 1.3 (m, 44H, 22  $\text{CH}_2$ ), 1.85 (m, 4H, 2  $\text{CH}_2$ ), 4.05 (t, 4H, 2  $\text{CH}_2\text{O}$ ), 7–9 (m, 20H, Ar).

## Experimental

The thermal behaviour was investigated using a Perkin–Elmer DSC7 differential calorimeter. The optical textures of the mesophases were observed through a polarizing microscope (Leitz Diavert) equipped with a hot stage (FP-82HT) and an automatic controller (Mettler FP-90). Samples are observed on regular slide glass without any surface treatment. X-Ray diffraction experiments were carried on a 18 kW rotating anode X-ray source (Rigaku-200) with use of Ge(111) crystal as monochromator. The scattered radiation was collected on a two dimensional detector (Imaging Plate system from Mar Research, Hamburg). The samples were placed in an oven, providing a temperature control of 0.1 K. Oriented samples of the smectic phases were obtained by slow cooling of a drop of the isotropic liquid. Electro-optical properties were studied using commercial cells (from E.H.C., Japan) with a rubbed polyimide layer (but the surface treatment is not effective to make uniformly oriented cells). Switching current was observed by applying a voltage-wave using a function synthesizer (HP 331 20A) and an high power amplifier (Krohn-Hite).

## Results and discussion

The transition temperatures and associated enthalpies are reported in Table 1. As frequently observed in banana series, the terminal chains greatly influence the occurrence of different “B” phases. Indeed, the dependence of the clearing points on the length of the alkoxy terminal chains suggests at least two regimes: the liquid crystalline–isotropic transition temperature  $T_{\text{cl}}$  first decreases increasing the number  $n$  of carbons in the terminal chains (from  $n=6$  to 10) and then slightly increases from  $n=11$  to 16. The assignment of the phases based on X-ray diffraction measurements and also on the optical observations and electrooptical studies confirms the existence of different B phases in the series depending on the carbon number in both terminal chains.

### Short homologues $S_6$ and $S_7$

These two compounds,  $S_6$  and  $S_7$ , possess two mesophases, one smectic phase and a two dimensional one at lower temperature. The smectic phase exhibits fan-shaped textures (Fig. 1a) like  $\text{SmA}$  but without any homeotropic tendency. The X-ray pattern of an oriented sample shows that this phase is a tilted smectic without in-plane order. The tilt angle is rather small (about  $10^\circ$ ). For these two compounds, the layer spacing is close to the half-length of the molecules ( $d=20 \text{ \AA}$  for  $n=6$  and  $20.8 \text{ \AA}$  for  $n=7$ ). These  $d$ -values suggest an intercalated structure. So this phase probably belongs to the B6 type. It should also be noted that this smectic phase does not show any electrooptical switching even at high voltages.

Decreasing the temperature, a two dimensional B1 phase<sup>1</sup> occurs. The transition is accompanied by a very low transition enthalpy ( $<0.2 \text{ kJ mol}^{-1}$ ) which suggests only subtle modifications of the molecular arrangement. An evolution of the textures towards a mosaic texture (Fig. 1b) is observed at the B6/B1 transition. The X-ray patterns show two reflections in the small angle region (Fig. 2) while in the wide-angle region a broad diffuse scattering indicates the liquid like order of the

**Table 1** Transition temperatures ( $^\circ\text{C}$ ) and enthalpies (italics,  $\text{kJ mol}^{-1}$ ) as a function of the carbon atom number in the terminal chains (from DSC runs, rate  $5^\circ\text{C min}^{-1}$ )

$n$	K	B1	B6	B2	I
6	• 120 <i>14.68</i>	• [115] <i>0.18</i>	• 160 <i>12</i>		•
7	• 120 <i>13.9</i>	• 139 <i>0.18</i>	• 146 <i>14</i>		•
8	• 120 <i>16.1</i>	• 135 <i>16.3</i>			•
9	• 113 <i>14.9</i>	• 123 <i>14.6</i>			•
10	• 117 <i>55.4</i>	• [113] <i>16</i>			•
11	• 104 <i>31.7</i>			• 112 <i>16.3</i>	•
12	• 109 <i>38.48</i>			• 114 <i>18.6</i>	•
13	• 109 <i>42.6</i>			• 116 <i>19.8</i>	•
14	• 111 <i>43.3</i>			• 118 <i>20.8</i>	•
15	• 114 <i>38.3</i>			• 118 <i>16.7</i>	•
16	• 108 <i>44</i>			• 119 <i>16</i>	•

<sup>a</sup>[ ] Indicates a monotropic transition.

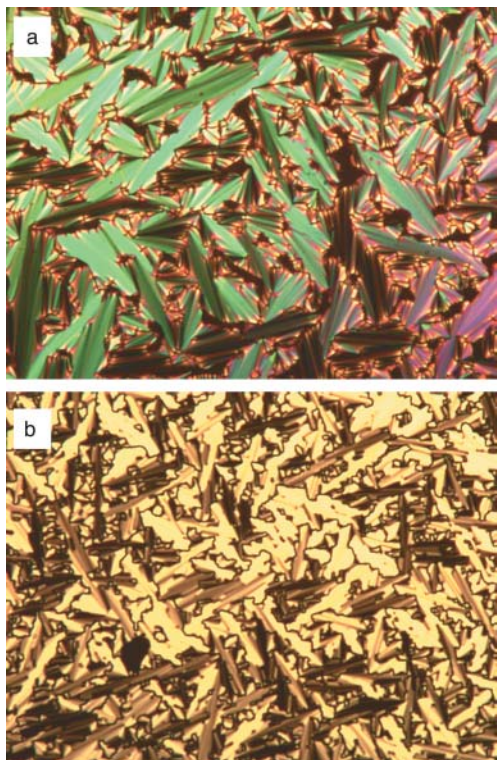


Fig. 1  $S_6$  homologue: a) 143 °C: B6 phase b) 102 °C B1 phase.

molecules within the layers. According to the indexing used in the literature for the B1 phase,<sup>15</sup> the two observed reflections can correspond to the 101 and 002 indices of a two-dimensional rectangular cell. Note that the 002 reflection in the B1 phase corresponds to the layer reflection in the B6 one.

### $S_8$ - $S_{10}$ homologues

On cooling from the isotropic liquid, the B1 phase of the  $S_8$ - $S_{10}$  homologues grows as dendritic nuclei which coalesce and give a mosaic texture (Fig. 3). X-Ray patterns are characterised by two reflections in the small angle region (Fig. 4). It is rather difficult to obtain a monodomain of the B1 phase, but in many cases, some oriented domains in the pattern clearly point to a two-dimensional lattice. According to a B1 assignment, one can assume a rectangular lattice with a parameter “ $c$ ” corresponding to the layer thickness (from the (002) reflection) and a parameter “ $a$ ” (from the (101) reflection) attributed to the in-plane periodicity of the modulated phase. The X-ray

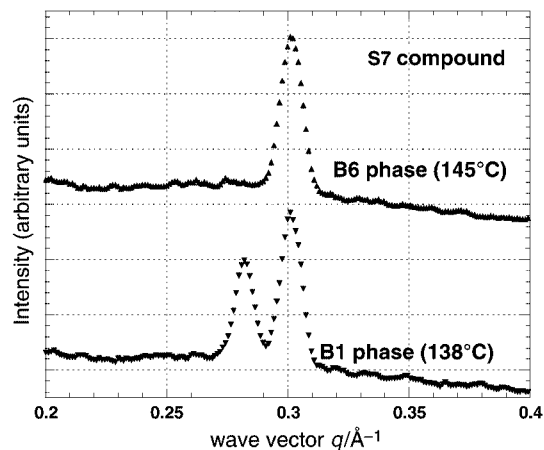


Fig. 2 Small angle X-ray scattering of the B6 (145 °C) and B1 (138 °C) phases of the  $S_7$  compound.

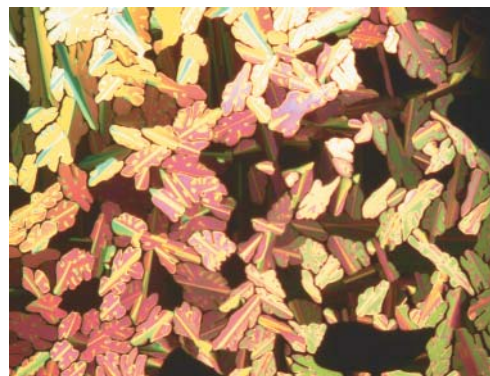


Fig. 3 Mosaic texture of the B1 phase of  $S_8$  compound (116 °C).

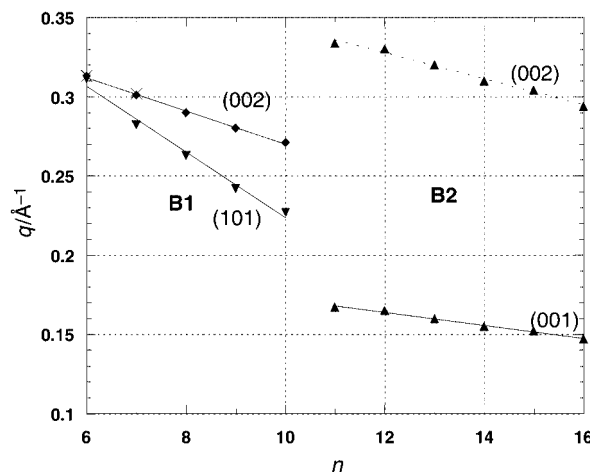


Fig. 4 Evolution of the wave vectors  $q$  ( $\text{\AA}^{-1}$ ) ( $q=2\pi/d$ , where  $d$  corresponds to the distance ( $\text{\AA}$ ) in real space) within the  $S_n$  series, in the B6, B1 and B2 phases. For  $S_6$  and  $S_7$  compounds, the crosses indicate the wave vectors corresponding to the layer reflections in the B6 phase. The Miller indices correspond to the B1 assignment.

data correspond to a low value of the “ $a$ ” parameter corresponding to a lattice involving very few molecules (for example  $a=23.2$  Å for  $S_6$ , 28.7 Å for  $S_8$  and 34.5 Å for  $S_{10}$ ).

### Long homologues $S_{11}$ - $S_{16}$

As in several series, the longer homologues exhibit a B2 phase. An example of the observed textures is given in Fig. 5 for the  $S_{16}$  compound and is similar to that exhibited by several standard compounds.<sup>1</sup>

The X-ray patterns of oriented samples indicate a tilted

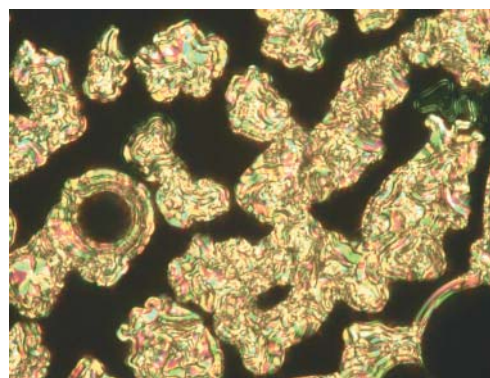
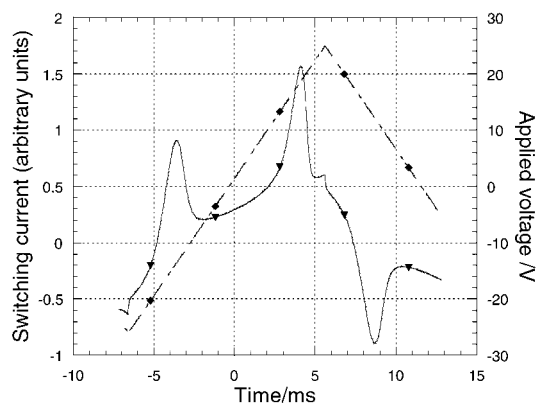
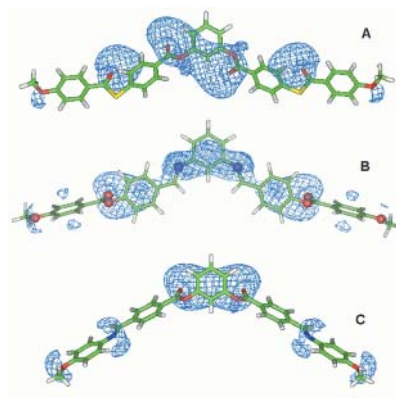


Fig. 5 Growth of the B2 phase on cooling from the isotropic liquid ( $S_{16}$  at 117 °C).



**Fig. 6** Switching current response in the B2 phase for the  $S_{16}$  homologue applying a triangular voltage ( $\pm 26$  V). Sample thickness  $3.3 \mu\text{m}$ , temperature  $100^\circ\text{C}$ .



**Fig. 7** Electrostatic potential maps of: (A)  $S_n$  series (B) series 7 of ref. 1 (C) PIMB series (ref. 1).

smectic. The layer spacing steadily increases from  $37.6 \text{ \AA}$  for  $S_{11}$  to  $42.7 \text{ \AA}$  for the  $S_{16}$  homologue (Fig. 4).

This phase shows an electro-optic response comparable with that of the B2 phase of several materials previously studied.<sup>1,7</sup> By applying a sufficiently high triangular voltage (above a threshold of  $1.5 \text{ V } \mu\text{m}^{-1}$ ), two current peaks can be recorded that point to “antiferroelectric” behavior (Fig. 6). The apparent saturated polarization  $P_s$  derived from the peak area is very high ( $800 \text{ nC cm}^{-2}$  for the  $S_{16}$  compound).

## Conclusion

In this new homologous series, including both short- and long-chained members, three banana mesophases have been evidenced: a B6/B1 dimorphism is observed for short compounds ( $n=6$  and  $7$ ), a sole B1 phase exists for intermediate aliphatic tail length ( $n=8-10$ ) and a switchable B2 phase occurs for long chains ( $n=11-16$ ). An analogous phase behaviour has been recently reported for a seven ring series<sup>16</sup> but up to now, this is the first example of five-ring banana-shaped compounds exhibiting the B6, B1 and B2 mesophases in the same series. Indeed, the B6 mesophase has been discovered for the hexyloxy compound of the series 7 of ref. 1 and the sole B1 phase is observed for heptyloxy to decyloxy homologues but the B2 mesophase could also exist for longer homologues which have not been synthesised.

In order to understand the physical parameters underlying the apparition of an intercalated structure, *i.e.* a B6 mesophase, we compare the repartition of the negative potential along the molecules of the two series ( $S_n$  and 7 of ref. 1) with those of reference compounds (PIMB series, see ref. 1) which do not exhibit a B6 mesophase. To this aim, we proceed as previously published:<sup>7</sup> the five-rings cores were built into MacroModel software version 6.5 (Schrödinger Inc.) and submitted to a Monte-Carlo conformational search. The lowest-energy conformations were selected and submitted to a semi-empirical quantum mechanics charge calculation (MOPAC/MNDO). The electrostatic potential maps (EPM) were drawn at the  $-40 \text{ kJ mol}^{-1}$  level (in blue, Fig. 7).

It is clear that the two series exhibiting a B6 mesophase (Fig. 7A and 7B) show a similar EPM pattern with three heavily loaded central rings. These patterns are quite different from those previously found in series exhibiting B2 and no B6 mesophases, with a strict alternation of positive and negative zones<sup>7</sup> (Fig. 7C).

Starting from the pattern 7A, it is possible to build a molecular arrangement of the  $S_n$  molecules by allowing an alternation of high and low potentials (see Fig. 8). In this case the periodicity appears as half the total length  $L$  of the molecule. The small rectangular boxes represent gaps which

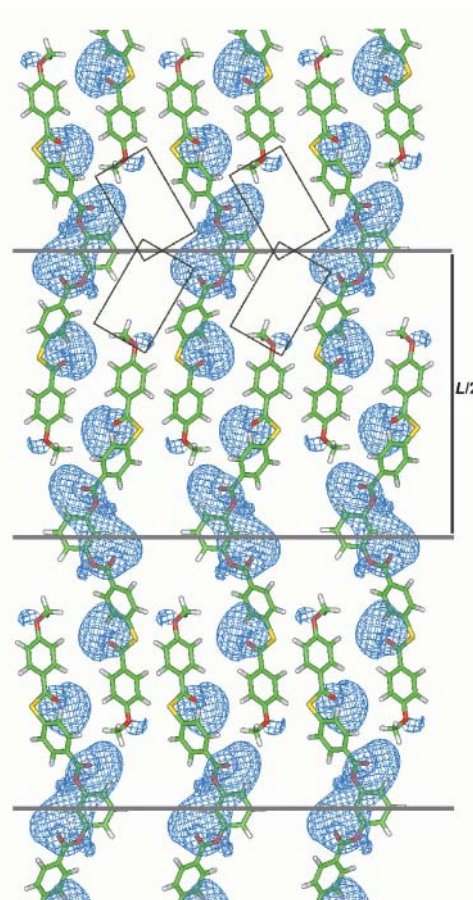


**Fig. 8** Possible local arrangement of the B6 phase. The rectangular boxes indicate the free space which can be filled by the aliphatic chains.

must be filled with slightly positive moieties, *i.e.* with the aliphatic chains. Due to the stacking constraints between the aromatic central cores, only rather short chains can accommodate the free room. This space is completely filled with a chain shorter than  $7 \text{ C}$ . This free space is not sufficient to accommodate longer chains and then the aliphatic chains may induce a lateral distortion of the structure giving rise to the rectangular cell of the B1 phase with similar local arrangement. The spatial arrangement of the B6 or B1 phases is no longer possible when the aliphatic tails contain more than  $10 \text{ C}$  and the whole structure topples toward a B2 arrangement with a periodicity close to the length of the molecule.

## References

- 1 See for example: G. Pelzl, S. Diele and W. Weissflog, *Adv. Mater.*, 1998, **11**, 707 and the references therein.
- 2 T. Niori, T. Sekine, J. Watanabe, T. Furukawa and H. Takezoe, *J. Mater. Chem.*, 1996, **6**, 1231.
- 3 T. Sekine, T. Niori, M. Sone, J. Watanabe, S. W. Choi, Y. Takanishi and H. Takezoe, *Jpn. J. Appl. Phys.*, 1997, **36**, 6455.
- 4 T. Niori, T. Sekine, J. Watanabe, T. Furukawa, S. W. Choi and H. Takezoe, *J. Mater. Chem.*, 1997, **7**, 1307.
- 5 S. Diele, S. Grande, H. Kruth, C. Lischka, G. Pezl, W. Weissflog and I. Wirth, *Ferroelectrics*, 1998, **212**, 169.
- 6 D. R. Link, G. Natale, R. Shao, J. E. MacLennan, N. A. Clark, E. Körblova and D. M. Walba, *Science*, 1997, **278**, 1924.
- 7 J. P. Bedel, J. C. Rouillon, J. P. Marcerou, M. Laguerre, M. F. Achard and H. T. Nguyen, *Liq. Cryst.*, 2000, **27**, 103.
- 8 J. P. Bedel, J. C. Rouillon, J. P. Marcerou, M. Laguerre, H. T. Nguyen and M. F. Achard, *Liq. Cryst.*, 2001, **28**(9), 1285.
- 9 G. Pelzl, S. Diele, A. Jakli, C. Lischka, I. Wirth and W. Weissflog, *Liq. Cryst.*, 1999, **26**, 135.
- 10 J. P. Bedel, J. C. Rouillon, J. P. Marcerou, M. Laguerre, H. T. Nguyen and M. F. Achard, *Liq. Cryst.*, 2000, **27**, 1411.
- 11 G. Heppke, D. D. Parghi and H. Sawade, *Ferroelectrics*, 2000, **243**, 269.
- 12 G. Heppke, D. D. Parghi and H. Sawade, *Liq. Cryst.*, 2000, **27**, 313.
- 13 D. M. Walba, E. Körblova, R. Shao, J. E. MacLennan, D. R. Link, M. A. Glaser and N. A. Clark, *Science*, 2000, **288**, 2181.
- 14 H. T. Nguyen, J. C. Rouillon, J. P. Marcerou, J. P. Bedel, P. Barois and S. Sarmiento, *Mol. Cryst. Liq. Cryst.*, 1999, **328**, 177.
- 15 J. Watanabe, T. Niori, T. Sekine and H. Takezoe, *Jpn. J. Appl. Phys.*, 1998, **37**, L139.
- 16 B. K. Sadashiva, V. A. Raghunathan and R. Pratibha, *Ferroelectrics*, 2000, **243**, 24.